# Comparison Between Radio Loud and Radio Quiet Fast CMEs: A Reason for Radio Quietness

M. Syed Ibrahim and E. Ebenezer

Kodaikanal Solar Observatory, Indian Institute of Astrophysics, Kodaikanal, Tamilnadu

## Introduction

- **Fast CMEs are mostly associated with magnetohydrodynamic (MHD) shocks in the solar orona, leading to the formation of type-II radio bursts.**
- **we aim to analyze the differences between the radio loud (RL) and radio quiet (RQ) fast Coronal Mass Ejections (CMEs) (speed 900 km s−1) during Solar Cycle 24 (2008-2021).**
- **From the 309 fast CMEs, we could identify 143 events that had a known source origin on the visible disk (Earth view). We identified the associated flares/CMEs for 143 events.**

## Data/Instrument

**(i) CME/Flare eruption region using Solar Dynamic Observatory /Atmospheric Imaging Assembly (SDO/AIA; Lemen et al. (2012)).**

**(ii) Large Angle Spectrometric Coronagraph (LASCO; Brueckner et al. (1995)) running-difference images to identify the CME-flare pair.**

**(iii) We focused on RL and RQ fast CMEs (speed 900 km s−1) during the Solar Cycle 24 .**

Table 1. The number of selected RL and RQ events during Solar Cycle 24 (2008 December-2021 August).

| Events | RQ | RL | Total |
|---|---|---|---|
| All | 70 | 73 | 143 |
| Accelerating CMEs | 17 | 24 | 41 |
| Decelerating CMEs | 53 | 49 | 102 |

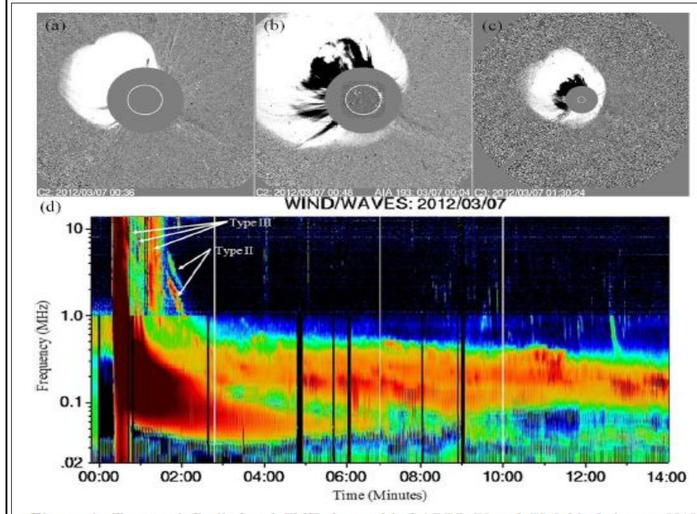


**Figure 1.** Top panel: Radio Loud CME observed in LASCO C2 and C3 field of view on 2012 March 7. Bottom panel: Wind/WAVES dynamic radio spectrum observations corresponding to the CME. Type-II and type-III radio burst signatures are indicated by the arrows.

Table 2. The statistics of flares of different classes associated with RL and RQ CMEs.

| Flare class | Number of CMEs | | |
|---|---|---|---|
| | All | Decelerating CMEs | Accelerating CMEs |
| Radio quiet | | | |
| X | 4 | 4 | 0 |
| M | 23 | 17 | 6 |
| C | 33 | 25 | 8 |
| B | 10 | 7 | 3 |
| Radio loud | | | |
| X | 16 | 13 | 3 |
| M | 40 | 26 | 14 |
| C | 17 | 10 | 7 |
| B | 0 | 0 | 0 |

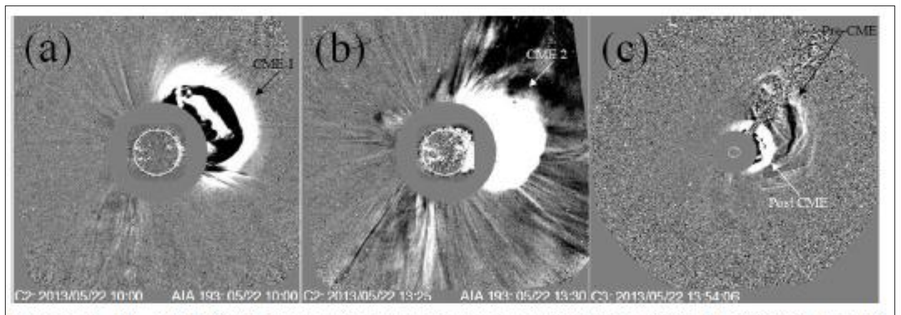


**Figure 5.** RL CME-CME interaction was observed on 2013 May 22 in LASCO C2 and C3 field of view. This RL CME interacted with pre-CME on the same date. The position of the post and previous CMEs are indicated by the black and white arrows in panel c.

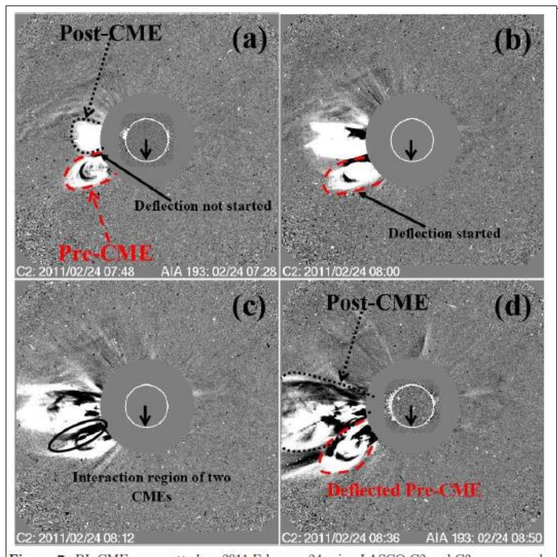


**Figure 7.** RL CME was spotted on 2011 February 24 using LASCO C2 and C3 coronagraphs (a)-(d). Interaction height of the CMEs, pre/post CME eruptions and deflection of the CME are mentioned.

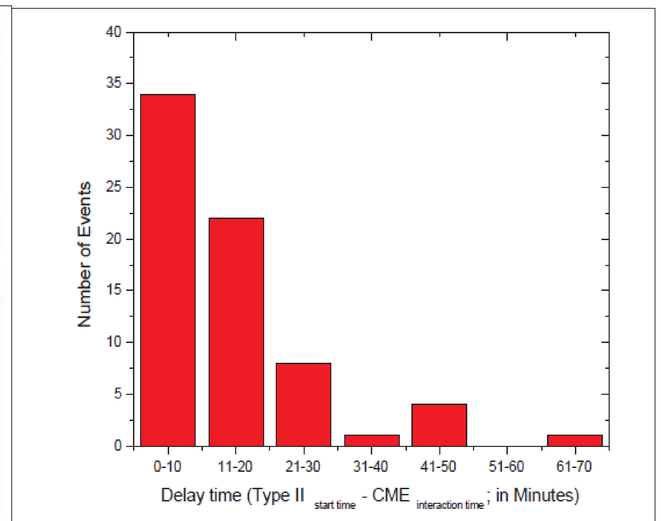


**Figure 6.** Distribution of the delay between DH type-II starting time and CME interaction time.

## References


- LASCO; Brueckner et al. (1995)).
- SDO/AIA; Lemen et al. (2012))
- Benz, Monstein, and Meyer (2005))
- Suresh and Shanmugaraju (2015).

Jang et al. (2016)


**Contact:**

**Ph:8489314781**

**mailID:syed.ibrahim@iiap.res.in**

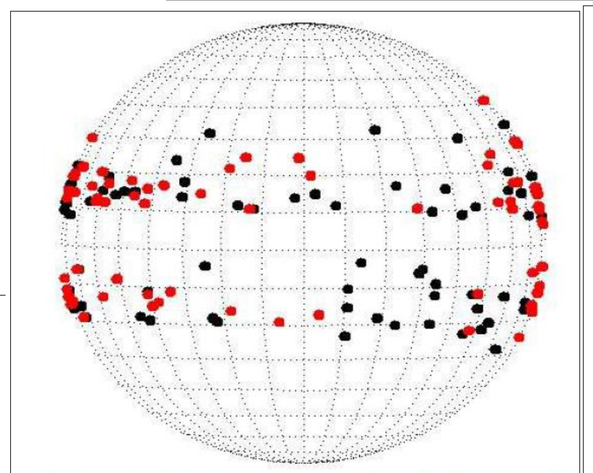

**Figure 3.** The heliogrphical original locations of RQ (red solid circle) and RL (black solid circle) associated CMEs.

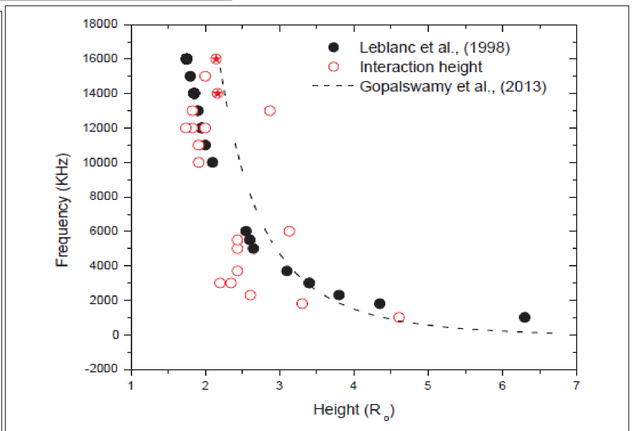


**Figure 8.** The height estimated from the starting frequency of DH type-II observations is compared to the height of the CME's interaction with any pre-CMEs or streamers. The Leblanc's one fold density model for heights between 2 and 7$R_{\odot}$ is shown by the solid circle.

**Result1:** **The observational evidence led to the conclusion that substantial density perturbation /interaction increases the probability of production of type-II radio emissions by shock of RL CMEs.**

**Result2: In the LASCO field of view, the majority of RL CMEs (almost 90%) interacted with streamers and/or pre-CMEs, whereas only 25% of RQ CMEs did the same, and there was no pre-CME interaction**